

NUMERICAL ANALYSIS OF A TWO-LAYER PCM BASED BATTERY THERMAL MANAGEMENT SYSTEM FOR DIFFERENT MATERIAL PROPERTIES

Bariş KAVASOĞULLARI^{1*}


¹Sivas University of Science and Technology, Faculty of Aviation and Space Sciences, Astronautical Engineering Department, 58000, Sivas, Türkiye

Abstract: The design and numerical analysis of the two-layer PCM (Phase Change Material)-based thermal management system for a 18650-type lithium-ion battery have been performed. In relation to simulation, the coefficient of thermal conductivity and melting temperature of the first layer of PCMs are varied. Other parameters are made identical to that of the next layer's parameters in order that the generation of two different layers of PCMs can be attained: PCM-1 and PCM-2. To obtain a more realistic approach in the numerical analysis, the battery thermal model was created in the COMSOL-MATLAB interface using the experimental internal resistance data obtained for 18650 type Li-ion batteries in the literature. While a cheaper and more accessible material with a thermal conductivity of 0.2 W/mK and a melting point of 50 °C was used in the PCM-2 layer, the thermal conductivity was changed as 0.2, 1 and 5 W/mK and the melting point was changed as 30, 40 and 50 °C in the PCM-1 layer. In this way, for PCM layers with different thickness (t_{pcm}), the system was optimized at two different discharge rates, 5C and 7C. As a result of the numerical analysis, it was determined that the optimum t_{pcm} , $k_{pcm,1}$ and T_m values for the 5C discharge rate were 2 mm, 0.2 W/mK and 40 °C, respectively; and the optimum t_{pcm} , $k_{pcm,1}$ and T_m values for the 7C discharge rate were 4 mm, 5 W/mK and 40 °C, respectively.

Keywords: Two-layer, Li-ion battery, Phase change material, Battery thermal management

*Corresponding author: Sivas University of Science and Technology, Faculty of Aviation and Space Sciences, Astronautical Engineering Department, 58000, Sivas, Türkiye

E mail: bkavasogullari@sivas.edu.tr (B. KAVASOĞULLARI)

Bariş KAVASOĞULLARI  <https://orcid.org/0000-0002-6086-8923>

Received: June 12, 2024

Accepted: October 17, 2024

Published: November 15, 2024

Cite as: Kavasogullari B. 2024. Numerical analysis of a two-layer PCM based battery thermal management system for different material properties. BSJ Eng Sci, 7(6): 1246-1255.

1. Introduction

With the knowledge that fossil fuels will run out in the near future, interest in electric vehicles is increasing day by day (Raijmakers et al., 2019). Although electric vehicles provide affordable, clean, and comfortable transportation, their performance and sustainability are largely dependent on the efficiency of the battery systems that power them (Barré et al., 2013). Lithium-ion (Li-ion) battery systems are widely preferred in electric vehicles due to their long cycle life, high power density and low weight (Zou et al., 2018). One of the most important disadvantages of Li-ion battery systems is that their performance and reliability are highly dependent on temperature (Kim et al., 2019). During their operation, high ambient temperatures and high charge/discharge rates can increase the battery temperature excessively. High temperatures can cause irreversible performance and life losses in the battery, and even serious reactions that can result in fire (Safdari et al., 2020). In many studies, safe temperature ranges for Li-ion battery systems have been specified as 50-60 °C (Ling et al., 2015; Kavasogullari et al., 2023). Battery thermal management systems (BTMS) have been developed to minimize the effects of temperature on the

battery and to keep the battery within reliable temperature ranges.

Phase change materials (PCM) are frequently preferred in battery thermal management systems due to their high latent heat (Yang et al., 2023; Moralı 2023). When these materials are applied in the battery pack, both good control of the battery cell temperature and uniform distribution of temperature throughout the battery pack can be achieved (Murali et al., 2021; Kavasogullari et al., 2024). In PCM-based battery thermal management systems, paraffin and its derivatives are widely used due to their relatively cheap and accessible nature (Maknikar and Pawar, 2023). On the other hand, the low thermal conductivity of these types of materials limits their use, especially under severe operating conditions (Luo et al., 2024). These types of materials act as insulation materials around the battery, especially after phase change, and cause heat to accumulate around the battery, thus causing the battery temperature to increase rapidly (Chen et al., 2024). To prevent this, some researchers have suggested adding certain amounts of nano-particle materials such as graphene, titanium oxide (TiO₂), iron oxide (Fe₂O₃) and alumina (Al₂O₃) into the PCM material (Talele and Zhao, 2023; Wang et al., 2024; Vyas



et al., 2024). Although PCM thermal conductivity can be significantly improved with this method, the added nanoparticles generally reduce the PCM latent heat (Radomska et al., 2020). In addition, since the addition of such materials to the PCM material requires an additional process and material, the system cost also increases. In order to increase the PCM performance by providing good thermal conductivity and to reduce the system cost, some researchers have proposed multilayer PCMs consisting of different PCMs. In their study, Kang et al. (2024) applied the three-layer PCM system to the battery pack and performed the numerical analysis of the system. As a result of the analysis, they reported that the three-layer PCM system reduced the battery temperature by 13.61 °C and the temperature difference in the battery pack by 2.54 °C compared to the system without PCM. Jilte et al. (2021) worked on two different types of designs for the two-layer PCM system, radial and longitudinal. As a result of the study, they determined that radial PCM layers provide better temperature control. In another study, Kang et al. (2023) performed the experimental and numerical analysis of longitudinal multilayer PCMs using graphene and paraffin. As a result of the study, they determined that the multilayer PCM system reduced the battery temperature by 32.6% at an ambient temperature of 20 °C and a discharge rate of 5C. Shivram and Harish (2024) numerically modeled a two-layer PCM system containing nanoparticles. The researchers used PCM with a melting point of approximately 27 °C in the first layer and a melting point of 82 °C in the second layer. As a result of the study, they revealed that adding nanoparticles shortens the PCM melting time and increases the heat transfer rate. As can be understood from the literature research, studies on multi-layer PCMs in BTMSs are quite limited. In this study, a two-layer PCM system in the radial direction was designed and its numerical analysis was performed. In the modeled system, the first layer used a PCM with a melting point of 30, 40 and 50 °C; the thermal conductivity coefficient was changed as 0.2; 1 and 5 W/mK, and the second layer used a PCM with a thermal conductivity coefficient and melting point kept constant at 0.2 W/mK and 50 °C, respectively. The PCM thicknesses were also changed to be the same as 2, 3 and 4 mm. In this way, it is aimed to reduce the system cost by using relatively cheaper and available PCM in the second layer. To ensure a realistic representation of the battery, a battery thermal model was created in COMSOL Multiphysics and MATLAB software using the battery properties obtained experimentally in the literature. In this way, BTMS was optimized at two different discharge rates, 5C and 7C.

2. Materials and Methods

The BTMS proposed in the study is shown in Figure 1. The system consists of a Li-ion battery cell and two separate PCM layers. In order to separate the PCM layers from each other and to keep the system together, an

aluminum shell with high thermal conductivity is placed between the layers and at the outermost part.

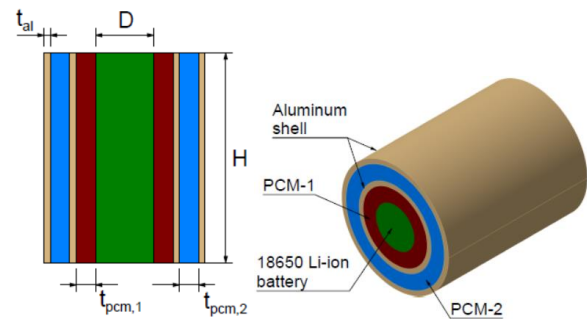


Figure 1. The modeled BTMS in the study.

In the BTMS analyzed, a 2.4 Ah capacity Li-ion battery of type 18650 ($D = 18$ mm and $H = 65$ mm) was considered (Lai et al., 2024). The heights of the PCM-1, PCM-2 and aluminum layers used in the system are equal to the battery height (H) and their thicknesses are determined as $t_{pcm,1}$, $t_{pcm,2}$ and t_{al} , respectively. $t_{pcm,1}$ and $t_{pcm,2}$ were changed within the scope of the analysis. t_{al} was taken as 1 mm to reduce thermal resistance. The thermophysical properties of the materials used are summarized in Table 1. As can be understood from the table, except for the melting temperature (T_m) and thermal conductivity (k_s and k_l), all other properties of PCM-1 and PCM-2 are the same. In the calculations, the k_s value of PCM-1 was changed to be 0.2; 1 and 5 W/mK, and the T_m value was changed to be 30, 40 and 50 °C. In PCM-2, the k_s and T_m values were kept constant at 0.2 W/mK and 50 °C, respectively. The thermophysical properties of the Li-ion battery and aluminum were taken from the COMSOL Multiphysics v6.2 software library (COMSOL, 2024).

2.1. Mathematical Modelling

The modeled system, as can be seen in Figure 1, consists of 18650 type cylindrical battery, PCM-1, Aluminum shell, PCM-2 and Aluminum shell layers from inside to outside. Here, a certain amount of current passes through the battery cell according to the given discharge rate and heat is generated due to its internal resistance. The heat released in the battery is absorbed by the PCM layers and the battery temperature is tried to be kept under control. When the heat absorbed by the PCM layers reaches a sufficient level, liquefaction occurs in the PCM. Accordingly, to determine the temperature and phase change behavior of the system, continuity, momentum and energy equations in all layers and phase change equations in PCM-1 and PCM-2 layers must be solved. The following assumptions were made to simplify the solution:

- Heat transfer by radiation is neglected.
- It is assumed that the system is completely insulated from the outside.
- It is assumed that the thermophysical properties of the battery, PCMs and Aluminum materials do not change with temperature.
- The battery cell used can be discharged at the 5C and 7C rates determined in the analysis.

Table 1. The thermophysical properties of the materials used in the study

Property	Definition	Li-ion cell (COMSOL 2024)	Aluminum (COMSOL 2024)	PCM-1 (El Idi et al. 2021)	PCM-2 (El Idi et al. 2021)
ρ_s , kg/m ³	Solid phase density	3600	2730	870	870
cp_s , J/kgK	Solid phase specific heat	881	893	2400	2400
k_s , W/mK	Solid phase heat conduction	1	155	0.2, 1.5	0.2
T_m , °C	Melting point	-	-	30, 40, 50	50
LH, kJ/kg	Latent heat	-	-	179	179
ρ_l , kg/m ³	Liquid phase density	-	-	760	760
cp_l , J/kgK	Liquid phase specific heat	-	-	1800	1800
k_l , W/mK	Liquid phase heat conduction	-	-	k_s	0.2
μ , Pa.s	Viscosity	-	-	0.00342	0.00342
β , 1/K	Thermal expansion coefficient	-	-	0.0005	0.0005

The conservation and phase change equations for the axisymmetric problem modeled in COMSOL Multiphysics software are given below. The energy equation for the battery side can be written as in equation 1:

$$\rho_b C_{p,b} \frac{\partial T_b}{\partial t} = k_b \nabla^2 T + \frac{Q_{gen}}{V_b} \quad (1)$$

Here ρ_b , $C_{p,b}$, k_b and V_b are the density, specific heat, heat transfer coefficient and volume for the battery, respectively. Q_{gen} is the heat generated in the battery and was described by Bernardi et al. (1985) with the following equation 2:

$$Q_{gen} = Q_{ir} + Q_{rev} \quad (2)$$

In equation 2, Q_{ir} and Q_{rev} are the irreversible and reversible heat amounts produced in the battery, respectively. Since Q_{ir} and Q_{rev} depend on the internal resistance, current and temperature, the total heat produced, Q_{gen} , can also be expressed by the following equation 3:

$$Q_{gen} = I^2 R - IT \frac{\partial U_{ocv}}{\partial T} \quad (3)$$

Here I , R , T and $\partial U_{ocv}/\partial T$ are the current (ampere), internal resistance (ohm), battery temperature (K) and short circuit voltage coefficient (V/K), respectively. In equation 3), the current I is found by multiplying the battery capacity with the discharge rate. In order to make a more realistic approach, the equations depending on temperature and SOC (State of charge) obtained experimentally by Lai et al. (2019) were used when finding the R value. The equations suggested by the researchers are presented below (equations 4a-e):

$$T = 293K: R = 166 - 1.334 \times SOC + 6.559 \times SOC^2 - 16.531 \times SOC^3 + 22.391 \times SOC^4 - 15.496 \times SOC^5 + 4.301 \times SOC^6 \quad (4a)$$

$$T = 303K: R = 107 - 793 \times SOC + 4.036 \times SOC^2 - 10.514 \times SOC^3 + 14.700 \times SOC^4 - 10.480 \times SOC^5 + 2.989 \times SOC^6 \quad (4b)$$

$$T = 313K: R = 66 - 382 \times SOC + 1.962 \times SOC^2 - 5.181 \times SOC^3 + 7.378 \times SOC^4 - 5.365 \times SOC^5 + 1.559 \times SOC^6 \quad (4c)$$

$$T = 323K: R = 58 - 355 \times SOC + 1.898 \times SOC^2 - 5.121 \times SOC^3 + 7.367 \times SOC^4 - 5.374 \times SOC^5 + 1.559 \times SOC^6 \quad (4d)$$

$$T = 333K: R = 48 - 233 \times SOC + 1.225 \times SOC^2 - 3.263 \times SOC^3 + 4.667 \times SOC^4 - 3.406 \times SOC^5 + 992 \times SOC^6 \quad (4e)$$

As can be seen above, the given equations were obtained for five different temperature values, 293, 303, 313, 323 and 333 K. For intermediate temperature values, interpolation was performed with the help of a MATLAB software code and the obtained internal resistance values were transferred to COMSOL software simultaneously. For temperature values greater than 333 K, the internal resistance value was calculated using equation 4e) as suggested by Lai et al. (2019). The short circuit voltage coefficient, $\partial U_{ocv}/\partial T$, was also calculated with the equation obtained experimentally in the same literature study (equation 5):

$$\frac{\partial U_{ocv}}{\partial T} = -0,355 + 2,154 \times SOC - 2,869 \times SOC^2 + 1,028 \times SOC^3 \quad (5)$$

The Q_{gen} value defined by equation 3 was calculated by

running equations 5, 4a, 4b, 4c, 4d and 4e simultaneously in COMSOL-MATLAB. The working method of the COMSOL-MATLAB couple is presented in Figure 2. As can be seen in the figure, in the first step, the T and SOC information was sent from the COMSOL software to the MATLAB code and then the R value was calculated in the MATLAB code and transferred to the COMSOL software. In the COMSOL software, the Q_{gen} value was determined using equations 5 and 3.

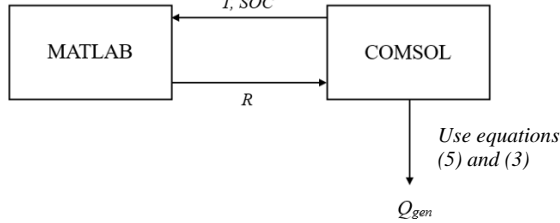


Figure 2. The calculation procedure of Q_{gen} .

For the axisymmetric system, continuity and momentum equations 6 and 7 in PCM layers can be written as follows (Samimi et al., 2016):

$$\frac{\partial \rho}{\partial t} + \frac{1}{r} \frac{\partial}{\partial r}(\rho r v_r) + \frac{\partial}{\partial z}(\rho v_z) = 0 \quad (6)$$

$$\rho \frac{\partial u}{\partial t} + \rho(u \cdot \nabla)u = -\nabla P + \rho \vec{g} + \nabla \vec{\tau} + \vec{F} \quad (7)$$

In the above equations, v and u are velocity components (m/s), g and τ are gravitational acceleration (9.81 m/s²) and shear stress (N/m²), respectively. In equation 7), F is the total volume force (N/m³) in the r and z directions and its value in the r direction will be $F_r = 0$. The component in the z -direction can be calculated with the following equation 8:

$$F_z = \rho g \beta (T - T_{ref}) \quad (8)$$

Here, T_{ref} is the reference temperature and is taken as 293.15 K. The energy equation for PCM is given in equation 9):

$$\rho C_p \frac{\partial T}{\partial t} + \rho C_p u \cdot \nabla T = \nabla \cdot (k \nabla T) \quad (9)$$

The effective thermophysical properties for PCM layers can be found with the following equations 10a-d:

$$k_{pcm} = \theta_1 k_s + \theta_2 k_l \quad (10a)$$

$$\rho_{pcm} = \theta_1 \rho_s + \theta_2 \rho_l \quad (10b)$$

$$C_{p,pcm} = \frac{1}{\rho_{pcm}} (\theta_1 \rho_s C_{p,s} + \theta_2 \rho_l C_{p,l}) + LH \frac{\partial \alpha_{pcm}}{\partial T} \quad (10c)$$

$$\alpha_{pcm} = \frac{1}{2} \frac{\theta_2 \rho_l - \theta_1 \rho_s}{\theta_1 \rho_s + \theta_2 \rho_l} \quad (10d)$$

Here, the subscripts s and l represent the properties in the solid and liquid phases, respectively, and are given in Table 1. α_{pcm} given in equation 10c is the PCM thermal diffusion coefficient (m²/s). θ_1 and θ_2 indicate

the ratio of solid and liquid materials in the PCM at any moment, respectively, and the sum of the two will be equal to one. Since heat transfer on the aluminum side will only occur by conduction, the energy equation 11 can be written as follows:

$$\rho C_p \frac{\partial T}{\partial t} - k \nabla T = 0 \quad (11)$$

2.2. Initial and Boundary Conditions

In order to solve the equations given above numerically, the initial and boundary conditions must be defined. Since the system is assumed to be completely isolated, the isolation boundary condition for all boundaries can be written as follows (equation 12):

$$-n \cdot q = 0 \quad (12)$$

In equation 12, n represents any coordinate. It is assumed that the temperature of the entire system is the same at $t = 0$. The relevant initial condition can be written as follows (equation 13):

$$t = 0; T_b(r, \Phi, z) = T_{pcm,1}(r, \Phi, z) = T_{al,1}(r, \Phi, z) = T_{pcm,2}(r, \Phi, z) = T_{al,2}(r, \Phi, z) = T_0 \quad (13)$$

Here, the initial temperature T_0 is taken as 20 °C. The conduction boundary conditions for the Battery-PCM-1, PCM-1-Aluminum, Aluminum-PCM-2 and PCM-2-Aluminum interfaces are given in equations 14, 15, 16 and 17, respectively.

$$k_b \frac{\partial T}{\partial n} = k_{pcm,1} \frac{\partial T}{\partial n} \quad (14)$$

$$k_{pcm,1} \frac{\partial T}{\partial n} = k_{al} \frac{\partial T}{\partial n} \quad (15)$$

$$k_{al} \frac{\partial T}{\partial n} = k_{pcm,2} \frac{\partial T}{\partial n} \quad (16)$$

$$k_{pcm,2} \frac{\partial T}{\partial n} = k_{al} \frac{\partial T}{\partial n} \quad (17)$$

2.3. Solution Procedure and Validation

In the numerical analysis performed in the study, COMSOL Multiphysics software was used to solve the conservation and phase change equations. Battery side thermal modeling in the system was performed with the COMSOL-MATLAB interface, considering the change of internal resistance with temperature. PCM temperature and phase change characteristics were determined using the "Heat Transfer in Solids and Fluids" module in the software. The momentum equations of PCM in the liquid phase were solved using the "Laminar Flow" module.

As stated in the previous section, the battery thermal model was created using the equations obtained in the literature study conducted by Lai et al. (2019). Before the analyzes performed within the scope of the study, the model created in the COMSOL-MATLAB interface

was verified with the same literature study. The results obtained in the verification analysis are shown in Figure 3. As shown, the COMSOL-MATLAB thermal model is highly consistent with the literature, with the maximum discrepancy determined to be 2%.

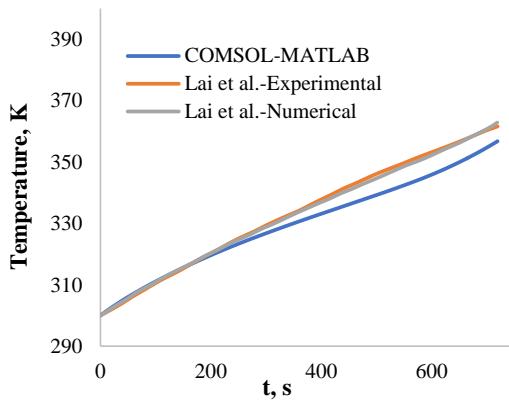


Figure 3. The validation of the COMSOL-MATLAB model created in the study with literature.

As is known, the mesh structure created in numerical studies also greatly affects the results. The mesh structure used in the numerical analysis performed in the study is shown in Figure 4. The mesh structure was prepared by dividing the calculation area into squares of a certain length. Since the mesh element dimensions are constant throughout the geometry, a mesh structure with an average element quality of 1.0 was obtained. The graph in Figure 5 shows the battery center temperatures obtained at 7C discharge rate with different mesh element dimensions. As can be seen in the graph, the temperatures obtained at the specified mesh element dimensions have almost never changed. Reducing the mesh element size will increase the total number of elements and therefore increase the calculation time. For this reason, the largest sized mesh element (2.5 mm) was preferred in the analyses performed to save time and energy.

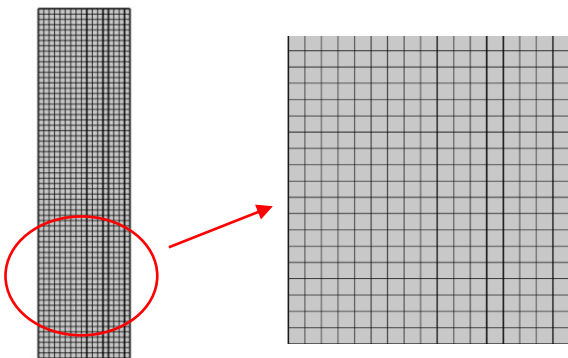


Figure 4. The mesh structure used in the numerical analysis.

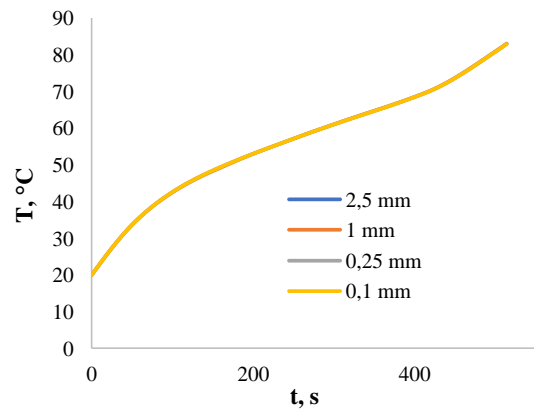


Figure 5. The temperature values obtained for different mesh element sizes.

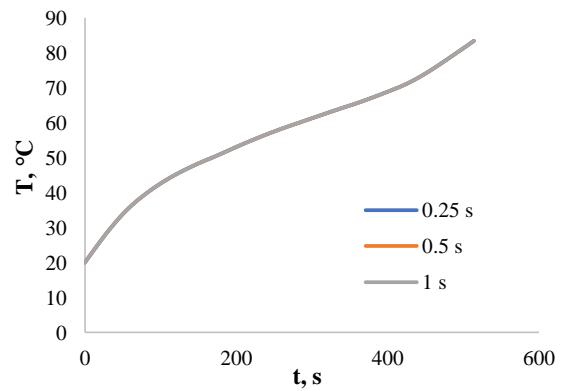


Figure 6. The results of time step size independence analysis.

Since the continuity, momentum and energy equations given in the study are time dependent, an analysis of independence from the time step size was also performed. In the analysis performed, numerical calculations were made for three different time step sizes, 0.25, 0.5 and 1 second. The battery core temperatures obtained at a discharge rate of 7C as a result of the calculation are shown in the graph in Figure 6. As can be seen in the figure, almost the same results were obtained for all determined time step sizes. Therefore, the time step size was taken as 1 second for an economical calculation.

3. Results and Discussion

In the presented study, as mentioned before, a two-layer PCM system with different properties was modeled. While the PCM with changing material properties was used in the first PCM layer (PCM-1), the material properties of the PCM in the second layer (PCM-2) were kept constant. Accordingly, the thermal conductivity of PCM-1 was changed as 0.2, 1 and 5 W/mK; and the melting point was changed as 30, 40 and 50 °C, while the other properties of PCM-1 were the same with PCM-2. The thermal conductivity of PCM-2 was taken as 0.2 W/mK and the melting temperature as 50 °C. In order to see the effect of the

PCM material thickness on the system performance, the t_{pcm} was changed as 2, 3 and 4 mm, which would be the same in both layers. In the created numerical model, the multilayer PCM system was subjected to discharge at two different speeds, 5C and 7C, and the discharge times for the determined discharge rates

were calculated as 720 and 514 seconds, respectively. The value reached by the battery center point temperature (T_b) at the end of the calculated discharge times was taken as the performance indicator in the system.

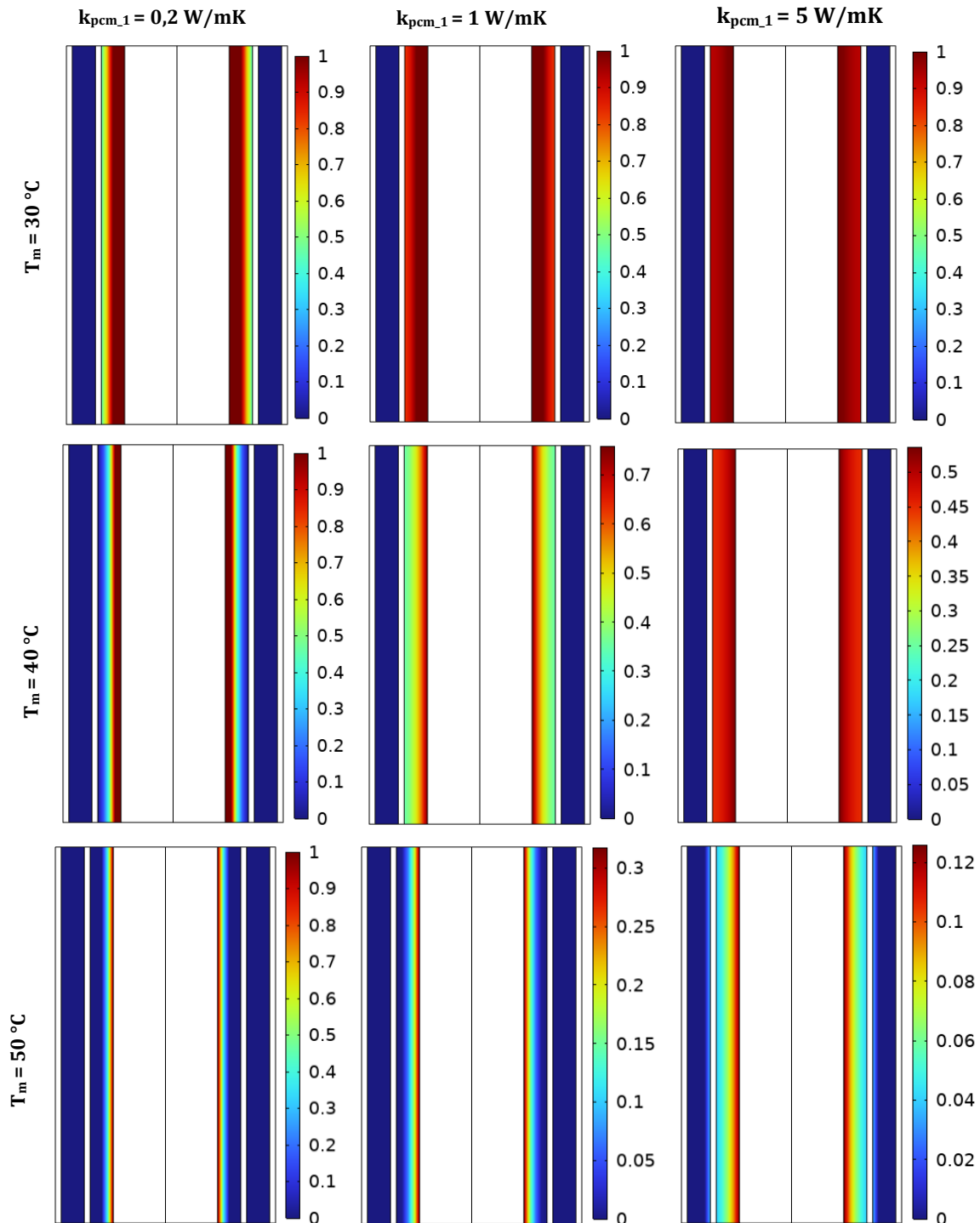


Figure 7. The liquefaction contours obtained for different $k_{pcm,1}$ and T_m values at 5C discharge rate ($t_{pcm} = 4 \text{ mm}$).

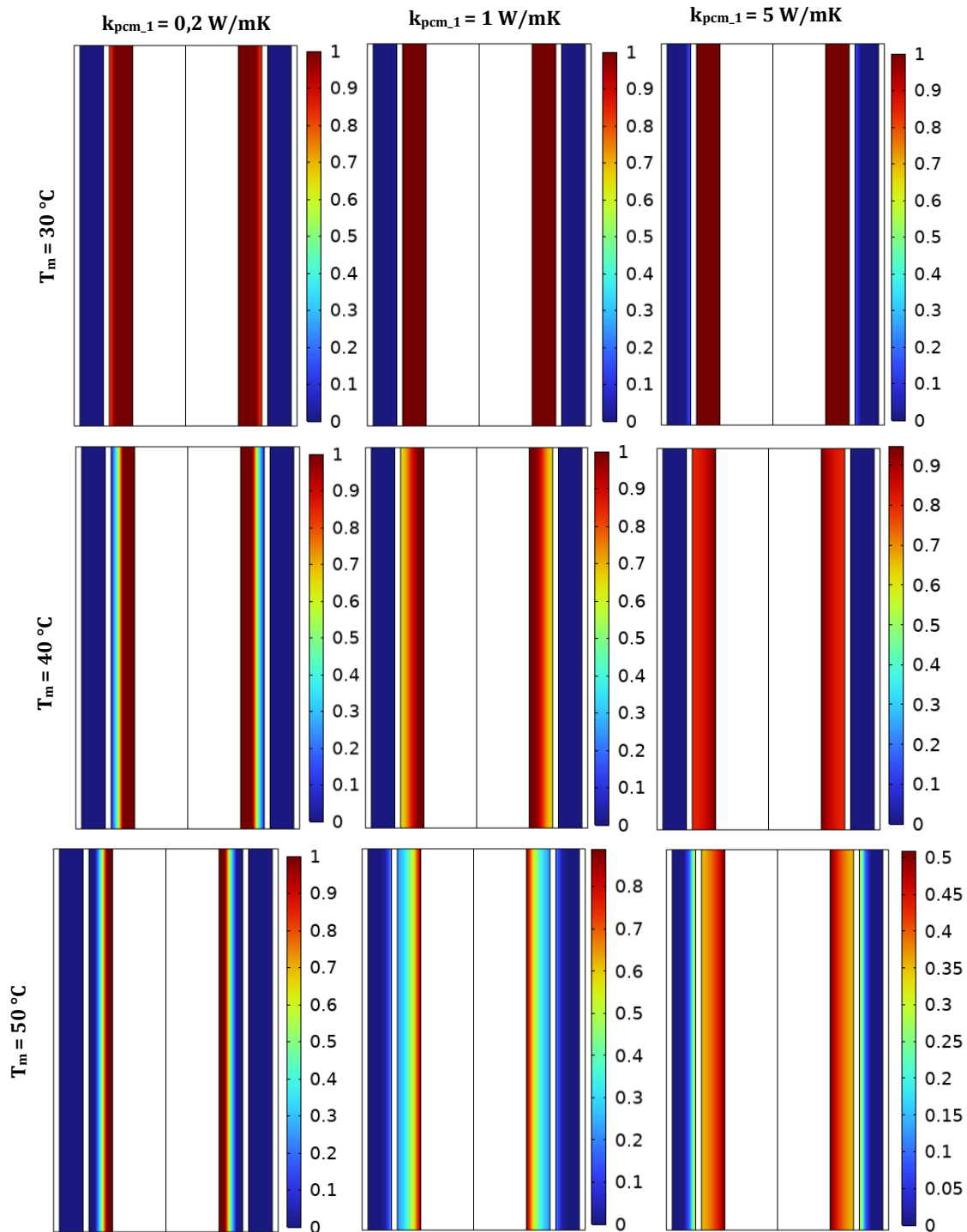


Figure 8. The liquefaction contours obtained for different $k_{pcm,1}$ and T_m values at 7C discharge rate ($t_{pcm} = 4$ mm).

The liquefaction contours obtained for different $k_{pcm,1}$ and T_m values for different 4 mm t_{pcm} at the end of the discharge time at 5C speed are shown in Figure 7. When different T_m values are examined, it is seen that almost no PCM-2 liquefied at $k_{pcm,1}$. In the system where only 5 W/mK PCM-1 was used, very little liquefaction occurred in PCM-2 at 50 °C. The reason for this is that the amount of heat generated in the battery at 5C discharge rate is relatively low. When different $k_{pcm,1}$ values are examined, it is determined that as the $k_{pcm,1}$ value increases, the amount of liquefactions in inner and outer layers of PCM-1 are closer to each other due to the improvement of heat

conduction, that is, the PCM-1 layer liquefied more homogeneously.

Figure 8 shows the liquefaction contours obtained at the end of the discharge period for different $k_{pcm,1}$ and T_m values for 7C discharge rate and 4 mm t_{pcm} . As can be understood from the figure, in the system using PCM-1 with 0.2 W/mK, PCM-2 almost did not melt at all T_m values. The reason for this is that at low $k_{pcm,1}$ values, heat could not be transmitted in PCM-1 and accumulates in the region close to the battery. While almost all of PCM-1 melted at all $k_{pcm,1}$ values for low T_m , increasing T_m value decreased the liquid ratio of PCM-1 and increased the

liquid ratio of PCM-2 at high $k_{pcm,1}$ values. At high $k_{pcm,1}$ values, heat could be transmitted more to PCM-2 layer and PCM-2 layer could be utilized more.

The battery temperature values obtained for T_m values at different thicknesses at 5C discharge rate are given in Figure 9. As can be understood from the graphs, especially at 0.2 W/mK $k_{pcm,1}$ value, increasing the thickness negatively affected the cooling performance of the system and caused the temperature to exceed 60 °C. Increasing the $k_{pcm,1}$ value at the same thickness improved the system performance. Considering the performance and cost parameters of the system, it was determined that using 0.2 W/mK PCM-1 with 2 mm thickness and 40 °C melting point is the most suitable solution.

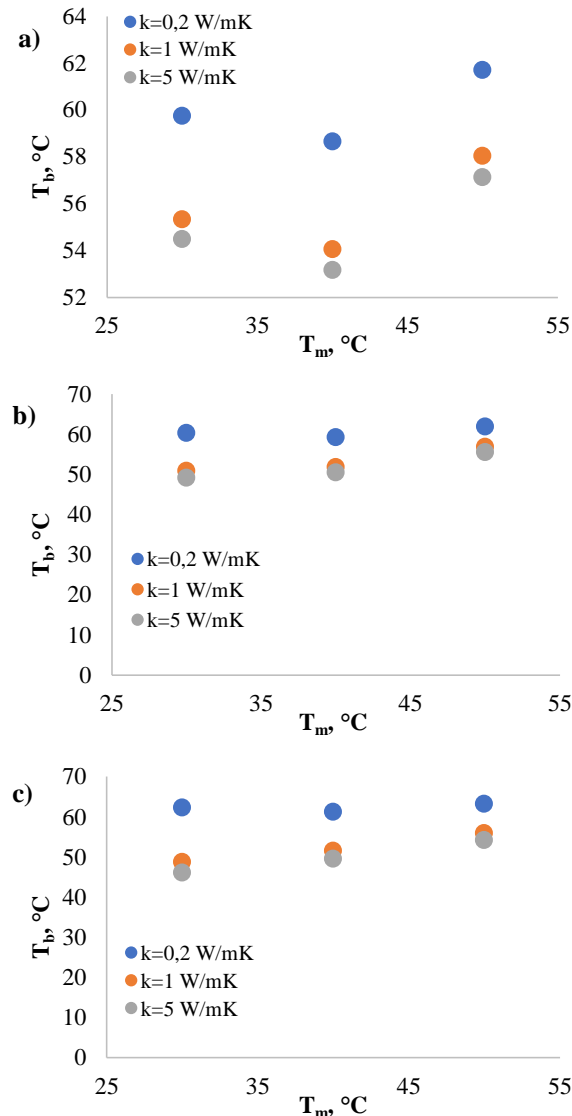


Figure 9. The battery temperature values obtained for different t_{pcm} and T_m values at 5C discharge rate: a) 2 mm, b) 3 mm and c) 4 mm.

Figure 10 shows the change of T_b values with T_m at 7C discharge rate for different $k_{pcm,1}$ values at 2, 3 and 4 mm thicknesses. As can be understood from the figures, as the $k_{pcm,1}$ value increased, T_b values decreased due to

better heat transfer to the PCM-2 layer. Increasing the thickness at low $k_{pcm,1}$ values caused T_b values to increase slightly. This can be caused by the greater accumulation of heat in the PCM-1 layer. When the T_m values are considered, at a $k_{pcm,1}$ value of 0.2 W/mK, the T_b value tended to decrease slightly as the T_m value increased. At higher $k_{pcm,1}$ values, T_b first decreased and then increased with the increase in the T_m value. Considering the obtained data, it was determined that the most suitable T_m value was 40 °C. Under the specified conditions, T_b was calculated below 60 °C for only 4 mm thickness, $k_{pcm,1} = 5$ W/mK and $T_m = 40$ °C. It was understood that PCM-1 and PCM-2 with a thickness of at least 4 mm should be used at the specified $k_{pcm,1}$ and T_m values for a safe discharge process.

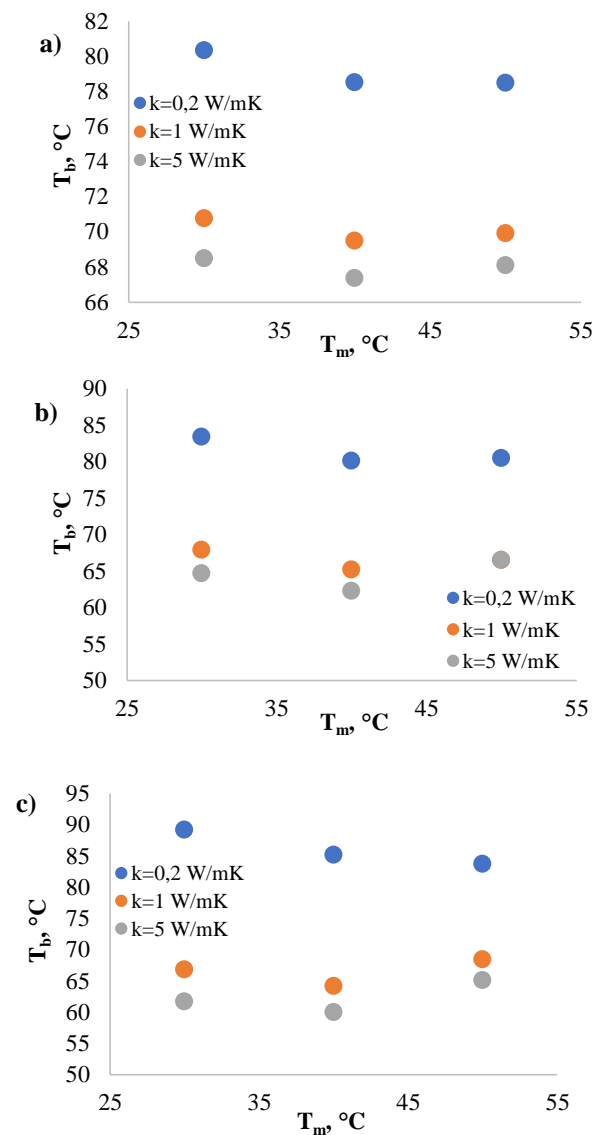


Figure 10. The battery temperature values obtained for different t_{pcm} and T_m values at 7C discharge rate: a) 2 mm, b) 3 mm and c) 4 mm.

4. Conclusion

In the presented study, numerical analysis of a BTMS using two-layer PCM was performed using COMSOL Multiphysics software. The thermal model of the 18650 type Li-ion battery in the system was created in the COMSOL-MATLAB interface using experimental data obtained in the literature. In the numerical analysis, two different PCM layers, namely PCM-1 and PCM-2, were obtained by changing the thermal conductivity ($k_{pcm,1}$) and melting point (T_m) of the PCM in the first layer. The system designed in this way was analyzed for two different discharge rates, 5C and 7C, different PCM layer thicknesses (2, 3 and 4 mm), different $k_{pcm,1}$ (0.2; 1 and 5 W/mK) and different T_m (30, 40 and 50 °C) values. The results obtained as a result of the analysis are summarized below:

- The liquefaction contours obtained for 4 mm t_{pcm} at 5C and 7C discharge rates showed that increasing the $k_{pcm,1}$ value provided more homogeneous liquefaction.
- For 4 mm t_{pcm} at 5C discharge rate, PCM-2 layer was almost not liquefied in all cases.
- When PCM-1 was used with 2 mm thickness, 0.2 W/mK and $T_m = 40$ °C in the system at 5C discharge rate, the battery temperature could be kept below 60 °C.
- At 7C discharge rate, the battery temperature could be reduced below 60 °C only when it was 4 mm thick, 5 W/mK and $T_m = 40$ °C. It was understood that PCM thickness should be at least 4 mm for a safe discharge at the determined rate.

Author Contributions

The percentage of the author contributions is presented below. The author reviewed and approved the final version of the manuscript.

	B.K.
C	100
D	100
S	100
DCP	100
DAI	100
L	100
W	100
CR	100
SR	100
PM	100
FA	100

C=Concept, D= design, S= supervision, DCP= data collection and/or processing, DAI= data analysis and/or interpretation, L= literature search, W= writing, CR= critical review, SR= submission and revision, PM= project management, FA= funding acquisition.

Conflict of Interest

The author declared that there is no conflict of interest.

Ethical Consideration

Ethics committee approval was not required for this study because there was no study on animals or humans.

References

- Barré A, Deguilhem B, Grolleau S, Gérard M, Suard F, Riu D. 2013. A review on lithium-ion battery ageing mechanisms and estimations for automotive applications. *J Power Sources*, 241: 680-689.
- Bernardi D, Pawlikowski E, Newman J. 1985. A general energy balance for battery systems. *J Electrochem Soc*, 132(1): 5.
- Chen G, Shi Y, Yu Y. 2024. A thermal management design using phase change material in embedded finned shells for lithium-ion batteries. *Int J Heat Mass Transfer*, 229: 125680.
- COMSOL Multiphysics® v. 6.2. www.comsol.com. COMSOL AB, Stockholm, Sweden.
- El Idi MM, Karkri M, Tankari MA. 2021. A passive thermal management system of Li-ion batteries using PCM composites: Experimental and numerical investigations. *Int J Heat Mass Transfer*, 169: 120894.
- Jilte R, Afzal A, Panchal S. 2021. A novel battery thermal management system using nano-enhanced phase change materials. *Energy*, 219: 119564.
- Kang C, Yang J, Yuan X, Qiu C, Cai Y. 2023. A novel multilayer composite structure-based battery thermal management system. *Front Energy Res*, 11: 1187904.
- Kang Z, Peng Q, Yin R, Yao Z, Song Y, He B. 2024. Investigation of multifactorial effects on the thermal performance of battery pack inserted with multi-layer phase change materials. *Energy*, 290: 130164.
- Kavasoğullari B, Karagöz ME, Yıldız AS, Biçer E. 2023. Numerical investigation of the performance of a hybrid battery thermal management system at high discharge rates. *J Energy Storage*, 73: 108982.
- Kavasoğullari B, Karagöz ME, Önel MN, Yıldız AS, Biçer E. 2024. Enhancing the performance of the hybrid battery thermal management system with different fin structures at extreme discharge conditions. *Numer Heat Transfer Part A: Appl*, 1-23.
- Kim J, Oh J, Lee H. 2019. Review on battery thermal management system for electric vehicles. *Appl Therm Eng*, 149: 192-212.
- Lai Y, Wu W, Chen K, Wang S, Xin C. 2019. A compact and lightweight liquid-cooled thermal management solution for cylindrical lithium-ion power battery pack. *Int J Heat Mass Transfer*, 144: 118581.
- Lai YW, Chi KH, Chung YH, Liao SW, Shu CM. 2024. Thermal runaway characteristics of 18650 lithium-ion batteries in various states of charge. *J Therm Anal Calorim*, 2024: 1-10.
- Ling Z, Wang F, Fang X, Gao X, Zhang Z. 2015. A hybrid thermal management system for lithium ion batteries combining phase change materials with forced-air cooling. *Appl Energy*, 148: 403-409.
- Luo T, Zhang Y, Chen X, Jia T, Yu H, Mao B, Ma C. 2024. A hybrid battery thermal management system composed of MHPA/PCM/Liquid with a highly efficient cooling strategy. *Appl Therm Eng*, 2024: 123617.
- Maknikar SK, Pawar AM. 2023. Application of phase change material (PCM) in battery thermal management system (BTMS): A critical review. *Mater Today Proc*, in press. <https://doi.org/10.1016/j.matpr.2023.08.329>
- Moralı U. 2023. A numerical and statistical study to determine the effect of thermophysical properties of phase change material for lithium-ion battery thermal management. *Numer*

- Heat Transfer Part A: Appl, 1-14.
- Murali G, Sravya GSN, Jaya J, Vamsi VNS. 2021. A review on hybrid thermal management of battery packs and its cooling performance by enhanced PCM. *Renew Sustain Energy Rev*, 150: 111513.
- Radomska E, Mika L, Szttekler K. 2020. The impact of additives on the main properties of phase change materials. *Energies*, 13(12): 3064.
- Raijmakers LHJ, Danilov DL, Eichel RA, Notten PHL. 2019. A review on various temperature-indication methods for Li-ion batteries. *Appl Energy*, 240: 918-945.
- Safdari M, Ahmadi R, Sadeghzadeh S. 2020. Numerical investigation on PCM encapsulation shape used in the passive-active battery thermal management. *Energy*, 193: 116840.
- Samimi F, Babapoor A, Azizi M, Karimi G. 2016. Thermal management analysis of a Li-ion battery cell using phase change material loaded with carbon fibers. *Energy*, 96: 355-371.
- Shivram S, Harish R. 2024. Impact of Dual Nano-Enhanced Phase Change Materials on Mitigating Thermal Runaway in Lithium-Ion Battery Cell. *Case Stud Therm Eng*, 104667.
- Talele V, Zhao P. 2023. Effect of nano-enhanced phase change material on the thermal management of a 18650 NMC battery pack. *J Energy Storage*, 64: 107068.
- Wang JX, Mao Y, Miljkovic N. 2024. Nano-Enhanced Graphite/Phase Change Material/Graphene Composite for Sustainable and Efficient Passive Thermal Management. *Adv Sci*, 2402190.
- Vyas D, Bhatt J, Rajput A, Hotta TK, Rammohan AR, Raghuraman DRSS. 2024. Investigation on Thermal Management of 18650 Lithium-Ion Batteries Using Nano-Enhanced Paraffin Wax: A Combined Numerical and experimental Study. *Arab J Sci Eng*, 1-18.
- Yang X, Deng G, Cai Z, Li H, Zeng J, Yang H. 2023. Experimental study on novel composite phase change materials with room-temperature flexibility and high-temperature shape stability in a battery thermal management system. *Int J Heat Mass Transfer*, 206: 123953.
- Zou D, Ma X, Liu X, Zheng P, Hu Y. 2018. Thermal performance enhancement of composite phase change materials (PCM) using graphene and carbon nanotubes as additives for the potential application in lithium-ion power battery. *Int J Heat Mass Transfer*, 120: 33-41.